Fluorescence Quenching Kinetics of Anthracene Covalently Bound to Poly(Methacrylic Acid): Midchain Labeling

John H. Clements and S. E. Webber*

Department of Chemistry and Biochemistry, The University of Texas at Austin, Austin, Texas 78712-1167

Received: November 6, 1998

Poly(methacrylic acid) labeled by anthracene in the middle of the chain (A-m-PMA) has been synthesized by anionic polymerization of *tert*-butyl methacrylate followed by introduction of the difunctional terminating agent 9,10-bis(bromomethyl)anthracene. Deprotection to yield the polyacid using trifluoroacetic acid in the presence of thioanisole results in complete removal of the *tert*-butyl moieties without destruction of the anthracene chromophore. Steady-state and time-resolved fluorescence quenching by Tl^+ in aqueous solution at pH 11 at different ionic strengths has been measured. The data have been analyzed and compared to data previously obtained for 9-ethanolanthracene pendant-labeled poly(methacrylic acid) (9EA-PMA) using the following kinetic models: Stern−Volmer; hindered-access; combined Stern−Volmer−Perrin model developed by Morishima et al. (*Macromolecules* **1993**, *26*, 4293). These two polymers exhibit very similar quenching behavior, with the most significant difference being that static quenching is more important for A-m-PMA than 9EA-PMA. The Morishima model has been modified to include a preferential binding constant (K_b) for Tl^+ in the vicinity of the chromophore. The estimated values of K_b are significant, on the order of 12−21, depending on the polymer and ionic strength.

Introduction

Polyelectrolyte-mediated chemical reactions have been the subject of considerable research.[1−3] An experimentally convenient example is fluorescence quenching of a polyelectrolyte-bound chromophore by ionic quenchers. It is well-known that the electrostatic potential of the polyelectrolyte plays a vital role in the enhancement or retardation of the quenching process. It is reasonable to expect that the efficiency of quenching will be strongly influenced by the precise location of fluorescence probes on the polymer. Morishima and co-workers have published numerous studies dealing with copolymers of sodium acrylate and acrylamide with pendant attachment of such probes as phenanthrene and 4-(4-hydroxyphenyl)ethenylpyridinium bromide.[4] In earlier work from these laboratories Morrison et al. have focused their attention on phenanthrene, anthracene, and diphenylanthracene pendant-tagged to poly(methacrylic acid).[2,3]

The typical synthesis of these polyelectrolytes utilized free radical copolymerization of the polyelectrolyte monomer with a low mole fraction of a monomer with the probe attached as a pendant group. The molar ratio of these components is chosen such that, on average, only a few chromophore-containing units are incorporated into each polymer chain, and the spatial distribution of chromophores on the polyelectrolyte chain is expected to be random. Anionic polymerization techniques have proven invaluable for the development of well-defined polymer−fluorophore systems. For instance, Hruska et al. found that this method reliably incorporated a single 1-(2-anthryl)-1-phenylethylene unit at the junction of a block copolymer of styrene and *tert*-butyl acrylate giving a well-defined pendant-tagged system.[5] Polymers tagged in this fashion have been used to elucidate the macromolecular environment in polymer micellar structures.[6] In this work, we report the anionic synthesis of poly(methacrylic acid) (PMA) labeled in the middle of the chain with a 9,10-dimethylanthracene probe and a study of the fluorescence quenching by Tl^+ as a function of ionic strength at pH 11. This pH is chosen to completely deprotonate the polymer so that we may concentrate on polyelectrolyte effects rather than the complex behavior of PMA as a function of pH.[7]

Poly(meth)acrylates as precursors for polyelectrolytes are attractive due to an extensive base of synthetic experience for these types of polymers. However, we have found that the subsequent hydrolysis or deprotection of the protected (meth)acrylates (e.g. methyl (meth)acrylate, *tert*-butyl (meth)acrylate) results in destruction of the polymer-bound 9,10-dimethylanthracene. We find that interception of the carbocation intermediate by thioanisole allows a successful deprotection scheme with little or no loss of this chromophore.

Experimental Section

I. Synopsis of Synthetic Scheme. Poly(*tert*-butyl methacrylate) was prepared by anionic polymerization in THF at −78 °C using cumylpotassium as the initiating species. The polymer was terminated by reaction with 9,10-bis(bromomethyl)anthracene resulting in the joining of two polymer chains through each dimethylanthracene junction. Low molecular weight material was removed by dialysis in acetone and the *tert*-butyl group removed by exposure to a trifluoroacetic acid/thioanisole mixture in the absence of oxygen.

II. Polymerization Reagents. *a. Solvent.* THF solvent was stirred over calcium hydride for 24 h and then twice treated with a sodium mirror to completely dry the solvent.

b. Monomer. *tert*-Butyl methacrylate monomer (Scientific Polymer Products) was passed through inactive alumina to remove inhibitor and predried by stirring over calcium hydride. After several hours of stirring, the monomer was cryodistilled and treated with diisobutylaluminum hydride followed by triethylaluminum. The light green color indicated the absence of moisture. The dry monomer was cryodistilled into a dry, sealed ampule and stored at 0 °C until needed.[8]

c. Initiator. Cumyl methyl ether was synthesized by reaction of 72.9 g (80.2 mL) of α-methylstyrene (1 equiv) with 50.0

10.1021/jp984343j CCC: $18.00
Published on Web 03/24/1999

mL of methanol (HPLC grade, 2 equiv) in the presence of 562 mg (338 μL) of 70% $HClO_4$. The mixture was allowed to stir at 50 °C under nitrogen for 48 h according to the procedure developed by Ziegler and Dislich.[9] To prevent polymerization during the course of the reaction, the *p-tert*-butylcatechol inhibitor present in the α-methylstyrene (Aldrich) was not removed. Chromatographic purification of the ether product was performed in pure hexane eluent in order to remove starting material and other impurities. The eluent was then gradually changed to pure ethyl acetate in order to recover the ether from the column. The collected solution was rotary evaporated to obtain the pure cumyl methyl ether product, which is a liquid. The liquid was stirred over calcium hydride to remove trace moisture and filtered. H NMR was used to confirm the absence of trace α-methylstyrene, indicated by olefinic doublets at δ 5.08 and 5.35 ($CDCl_3$). H NMR: δ 1.57 (s, $-C(CH_3)_2$), 3.10 (s, $-OCH_3$), 7.25−7.48 (complex, 5 × Ar H).

Cumyl potassium was synthesized from 0.70 g of cumyl methyl ether (1 equiv) under reduced pressure in the presence of 0.40 g of potassium metal (mirror, 2.2 equiv) and 100 mL of THF solvent.[9] Upon exposure of the ether to the potassium mirror a deep red color was observed, indicating the presence of the cumyl anion. The mixture was allowed to stir for 24 h at room temperature and in the absence of light. Note that this method does not produce the fluorescent impurities reported by Winnik and co-workers.[10] The concentration of the deep red initiating species was determined by titration with dry acetanilide and usually found to be near 40 mM. The cumylpotassium solution was transferred to an ampule and used as soon as possible because it tends to form unidentified side products if stored for more than 96 h even if light exposure is kept to a minimum.

d. Terminating Agent: 9,10-Bis(bromomethyl)anthracene. 9,10-Bis(chloromethyl)anthracene (Aldrich) was used without further purification. A total of 3.0 g (1 equiv) of 9,10-bis(chloromethyl)anthracene solid was extracted into a solution of 6.0 g (5.3 equiv) of sodium bromide in 220 mL of acetone using a Soxhlet apparatus and allowed to reflux under nitrogen for 18 h, following the procedure developed by Golden.[11] Due to the photoreactive nature of the product, the material was protected from room light exposure during the reaction and subsequent purification process. The reaction mixture was cooled to room temperature and filtered. The yellow residue, which was mostly monobrominated material, was collected and extracted a second time in the presence of sodium bromide using toluene solvent to yield the desired dibrominated species. The final residue was collected, recrystallized from toluene, and freeze-dried as an emulsion in benzene to yield pure, dry 9,10-bis(bromomethyl)-anthracene (9,10-DBMA). Note that purification via chromatography using alumina or silica stationary phases results in decomposition of the product into a variety of species as detected by TLC. MS: *m/z* 367 (M^+), 366, 365, 364, 363, 285, 283, 205. H NMR: δ 5.50 (s, 2 × $-CH_2-$), 7.63−7.70 (m, 2,3,6,7-H), 8.32−8.40 (m, 1,4,5,8-H). MP: >300 °C in agreement with Golden.[11]

e. Preparation of Terminating Solution. 9,10-DBMA was placed in a dry, clean round-bottom and exposed to vacuum. High-purity THF was cryodistilled to dissolve the fluorophore followed by cryodistillation to dryness in order to entrain off any trace moisture left in the original solid sample. This process was repeated once followed by a final dissolution in a minimal amount of THF to achieve the pure terminating solution used for the polymerization (∼3−4 mg/mL concentration). This solution was transferred to a dry, sealed ampule via cannula.

SCHEME 1

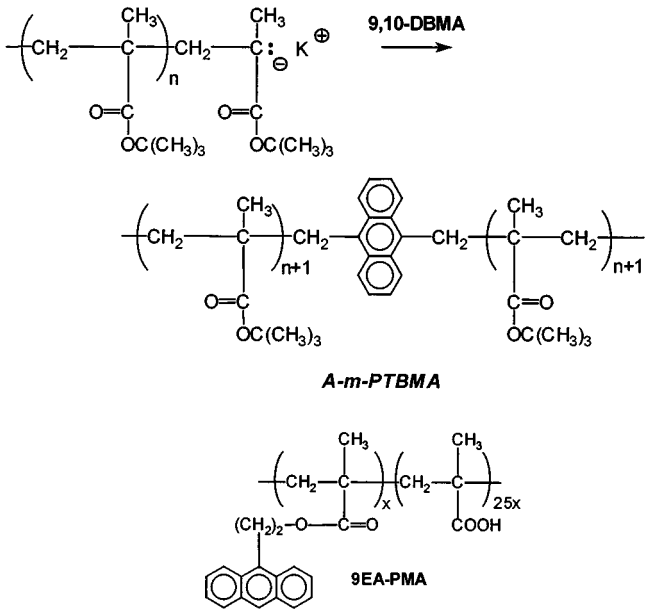

III. Preparation and Termination of Polymer. The polymerization reactor was assembled, evacuated, and flame-treated, after which approximately 250 mL of THF was cryodistilled into the vessel at −78 °C followed by pressurization with high-purity nitrogen. The cold THF was allowed to warm to near room temperature at which time existing impurities in the solvent were eliminated by titration with initiator solution. The persistence of a light peach color was indicative of a dilute solution of unreacted cumylpotassium and signified the end point of the titration. The vessel was again cooled to −78 °C, and the appropriate amount of initiator solution was added and allowed to mix thoroughly. Monomer was added dropwise to the vigorously stirring solution in order to suppress the premature termination mechanism discussed by Warzelhan et al.[12] in which free monomer may undergo nucleophilic attack by the living chain end, thereby terminating the chain and eliminating a methoxy anion. After 1 h a small aliquot of the polymer solution was isolated for subsequent study via a glass siphon and terminated with methanol. A total of 0.40 equiv of 9,10-DBMA in THF was then added to the vessel and allowed to react with the living chain ends for 1.5−2 h at −78 °C (Scheme 1). The mixture was then slowly warmed to room temperature for an additional 1 h to ensure completion as described by Valeur and co-workers.[13] At this stage, any chains that might still be living were quenched with methanol. The resulting anthracene mid-tagged poly(*tert*-butyl methacrylate) (A-m-PTBMA) was purified and analyzed according to the procedures detailed below.

IV. Purification of Polymer. Dialysis was employed as an effective method to remove any unreacted terminating fluorophore as well as other impurities from the polymer. A concentrated solution of A-m-PTBMA in acetone (∼10 mg/mL) was prepared. This was placed into a Spectra/Por series 1 cellulose membrane tubing with a molecular weight cutoff of 6000−8000 which was sufficient to allow low molecular weight impurities to pass while retaining the polymer. The solution was dialyzed against an outer acetone solution that was changed every 3−4 h until the presence of impurities migrating into this solution could no longer be detected by UV−vis absorption spectroscopy. This procedure usually involved 8−10 outer solution changes. Note that, prior to use, the membrane tubing was immersed in 5% acetic acid solution for 10 min to remove trace metals and then conditioned to acetone environment by a

30−45 min soaking in pure water followed by similar soakings in water/acetone mixtures of progressively higher acetone content. This procedure is extremely important since sudden immersion into organic solvents can warp membrane pores. The A-m-PTBMA solution retained inside the membrane tubing was evaporated, the polymer was dissolved in dioxane, and the solution was filtered and freeze-dried.

V. Deprotection of Polymers. *a. Untagged PTBMA.* A 125 mg amount of polymer was dissolved in 75 mL of dioxane. To this was added 250 μL of concentrated (37 wt %/wt) HCl (3.5 equiv/acid residue), and the resulting mixture was allowed to stir at 85−90 °C for 8 h. Because the acid-catalyzed elimination reaction produces volatile isobutylene and no other side products, the mixture was filtered and freeze-dried without further purification. Complete elimination of the *tert*-butyl group was confirmed by H NMR (see next section).

b. A-m-PTBMA. A 250 mg amount of A-m-PTBMA was dissolved in 10 mL of methylene chloride. This solution was placed in a clean, dry round bottom and degassed on a high vacuum system. To this was cryodistilled 3 mL of thioanisole (15 equiv) followed by 10 mL of trifluoroacetic acid (75 equiv) Each had previously undergone three freeze−pump−thaw cycles in order to remove the dissolved oxygen. The resulting ∼45% trifluoroacetic acid (TFA) mixture was allowed to react on the high vacuum system in the absence of room light for 1 h at 50 °C and at reduced pressure. The solvents were then cryodistilled away. Dioxane (3 freeze−pump−thaw cycles) was cryodistilled into the round-bottom flask to redissolve the polymer, followed by cryodistillation to dryness in an effort to remove the *tert*-butyl trifluoroacetate which is formed during the course of the reaction. Note that this method is similar to the entrainment procedure used to remove trace moisture from the 9,10-DMBA terminating species.

A second 3 mL aliquot of thioanisole followed by 10 mL of TFA was cryodistilled into the reaction vessel, and this ∼75% TFA mixture was allowed to react with the partially deprotected polymer for an additional 1 h at 50 °C to complete the reaction. Two successive entrainments with dioxane were performed (similar to the procedure described above) to remove TFA, *tert*-butyl trifluoroacetate, and thioanisole. The polymer residue was then exposed to vacuum at room temperature to remove remaining traces of thioanisole and freeze-dried in dioxane to obtain pure anthracene mid-tagged poly(methacrylic acid) (A-m-PMA). Note that removal of thioanisole is crucial prior to freeze-drying because it depresses the freezing point. Even small amounts of thioanisole will greatly reduce the effectiveness of the freeze-drying process, which is essential in order to obtain the final polymer as a dry powder. The extent of elimination of the *tert*-butyl group was determined by comparison of the integral values at δ 1.39 (s, $-C(CH_3)_3$) and 1.60−2.20 (complex, $-CH_2-$) in methanol-*d* and was found to be complete within the limits of NMR detection (1%).

VI. Instrumentation and Analytic Techniques. *a. Nuclear Magnetic Resonance.* All NMR measurements were performed on either a Bruker AC-250 (250 MHz) or a Varian (300 MHz) spectrometer.

b. Gel Permeation Chromatography. Purity, extent of tagging, and molecular weight distribution of the polymer products was assessed on a gel permeation chromatography (GPC) system consisting of a model 510 Waters pump connected to a series of four Waters Millipore μStyagel columns (10^5, 10^4, 10^3, and 500 Å, in order of flow) using UV−vis absorption, fluorescence, and refractive index detectors, sequentially. A Hewlett-Packard Vectra 486DX4-100 computer controlled a HP 1050 diode array detector and was equipped with an A/D board to simultaneously record the analogue output from the Waters R401 differential refractometer and the Perkin-Elmer LS-1 fluorescence detector. THF was used as the mobile phase at a flow rate of 1.5 mL/min. Polystyrene standards (Scientific Polymer Products) were used for calibration.

For each chromatogram the optical density at 230 nm (polymer absorption) and 380 nm (anthracene absorption) was obtained as a function of elution volume. The chromatograms were saved as Borland C++ v2.0 based executable files for calculation of molecular weight averages and polydispersities.[14] GPC analysis of polyacid required methylation of −COOH groups by diazomethane.[15]

c. Fluorescence Measurements. Steady-state and time-resolved measurements were performed on a SPEX DM3000 Fluorolog-τ2 spectrofluorometer equipped with a 450 W xenon light source, Czerny-Turner double monochromators for excitation and emission, and Hamamatsu R928-P emission and reference (rhodamine-B) photomultipliers. A potassium dideuterium phosphate crystal was used to modulate the light source for time-resolved phase modulation experiments. These time-resolved measurements were referenced with an aqueous glycogen scattering solution ($\tau_{ref} = 0$). Lifetime data were obtained using a modulation frequency range of 10−150 MHz. Subsequent analysis was performed using SPEX Globals Unlimited Version 2.1 software. Decays were fit to a sum of exponentials using the Marquardt minimization method for χ^2.

VII. Quenching Experiments. *a. Stock Solutions.* A known amount of A-m-PMA was placed into a clean, dry volumetric flask. To this was added a predetermined amount of standardized 0.1 M KOH (titrated against potassium hydrogenphthalate) to give a final solution with pH 11.00, taking into account the appropriate amount necessary for complete ionization of the polyacid. After final dilution of the polymer solution with deionized water to yield a methacrylic acid residue concentration of approximately 1.5 mM, the pH was measured. The pH value obtained was almost always higher than that calculated (probably due to partial ionization of the original polymer powder) but never exceeded 11.25. Due to the observation of a systematic change in the fluorescence spectrum as a consequence of prolonged room light exposure, the solution was protected from light during storage, which was not allowed to exceed 1 week due to measurable drops in the pH from day to day.

The thallium(I) heavy-atom quencher was chosen for these studies because of its similarity in size to the potassium counterion.[3] Solutions of $TlNO_3$ in water were prepared with concentrations ranging from 40 to 250 mM depending on the quencher concentration region of interest. The dependence of the quenching efficiency on ionic strength was investigated by addition of small amounts of a KNO_3 stock solution. The concentrations of these solutions were chosen such that their addition to give the highest quencher and salt concentrations studied resulted in no more than a 10% increase in the polymer solution volume. Note that we have defined the ionic strength (IS) of the solution in the following manner:

$$IS = [KOH] + [KNO_3] - {}^1/_2[COO^-] \qquad (1)$$

where $[COO^-]$ refers to the concentration of methacrylic acid residues and is included to take into account neutralization of hydroxide ions during ionization of the polymer. All solutions were purged with N_2 bubbling for 15 min prior to usage.

b. Steady-State Measurements. 2.600 mL volume of the A-m-PMA stock solution was placed into a quartz cuvette, equipped with screw cap containing gas inlet/outlet, and the solution

SCHEME 2

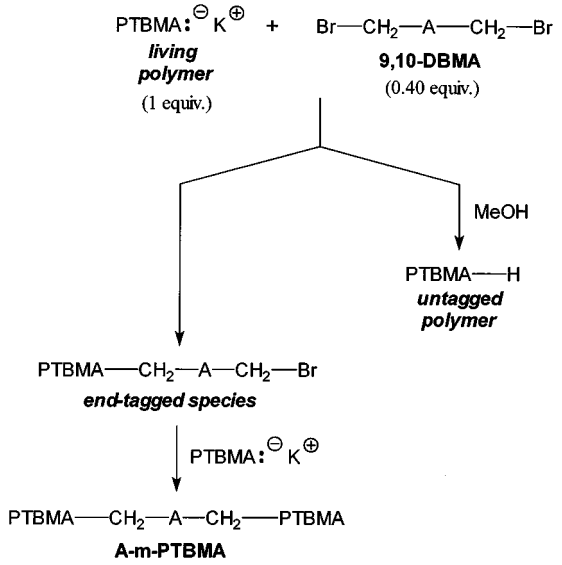

bubbled with nitrogen for 15 min. Excess salt was added at this time to achieve the desired ionic strength and the solution allowed to mix. The sample was excited at 383 nm and the emission recorded from 395 to 520 nm with the signal referenced to the excitation intensity (the S/R mode). Small amounts of quencher stock solution (~3−10 μL) were added between each subsequent run and allowed to mix for 2−3 min with N_2 bubbling prior to the acquisition of the spectrum. Dilution of the fluorophore by addition of quencher and salt solutions was taken into account in later analysis.

Results

I. Tagging of Polymers. It is essential that the mid-tagged product not contain any end-tagged material. This could be the case if the chains displace only one bromine of 9,10-DBMA, which results in an end-tagged polymer with half the molecular weight of the desired product (Scheme 2). The presence of an unwanted end-tagged species would necessitate removal by GPC, resulting in the purification of only small quantities of material, as reported by Sasaki et al. for this type of polymer.[16] Therefore, we added a substoichiometric ratio of 9,10-DBMA to the living polymer chains. When the chromatograms monitored at 230 and 380 nm are compared, it is evident that the anthracene is associated only with the doubled molecular weight polymer (Figure 1a,b). In addition, the 230 nm trace of the polymer aliquot taken before 9,10-DBMA termination (Figure 1c) has only a small overlap with the 380 nm trace of the tagged polymer further suggesting the absence of any end-tagged material. Furthermore, close inspection of the 380 nm trace of the tagged material shows no low molecular weight tail or shoulder that would normally be associated with the presence of a small fraction of tagged low molecular weight polymer. Analysis of the GPC traces demonstrated that the tagged species molecular weight (M_n) was 37 500 (target: 40 000), PD = 1.09, and there was an untagged species of approximately half the molecular weight. Analysis of the polymer aliquot taken before 9,10-DBMA termination yields M_n = 15 300, PD = 1.10.

II. Deprotection of Polymers. Deprotection of poly(meth)-acrylates has been discussed by many researchers. Dissolution of PTBMA in toluene followed by mild heating (~80 °C) in the presence of *p*-toluenesulfonic acid has been shown to yield the deprotected product,[17] while Kamachi and co-workers have shown that prolonged exposure to H_2SO_4 at ambient temperature is effective in deprotecting a variety of (meth)acrylates.[18] The

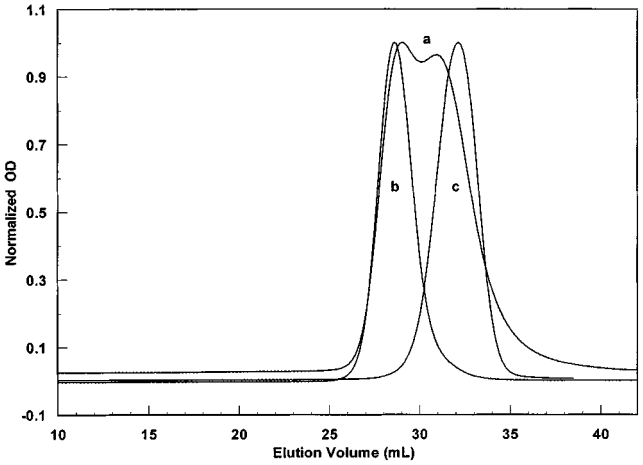

Figure 1. Comparison of the absorption at 230 nm (a) and 380 nm (b) GPC trace for A-m-PTBMA with the 230 nm absorption GPC trace for the untagged aliquot (c).

SCHEME 3

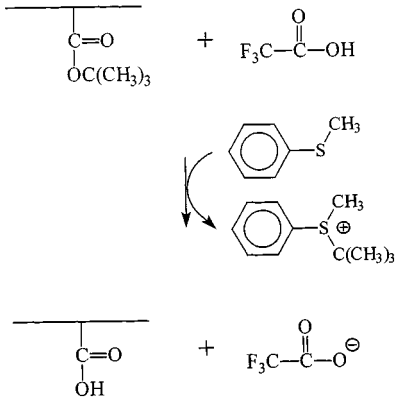

HCl/dioxane method described in the Experimental Section, employed by Procházka et al., has been our standard method for deprotection of untagged PTBMA.[19]

Deprotection of A-m-PTBMA proved much more difficult. Upon exposure of the mid-tagged material to the HCl/dioxane mixture, a nearly complete (>99%) loss of anthracene fluorescence and absorption (>300 nm) was observed. Furthermore, H NMR found that only 89% of all residues were deprotected. In light of these findings, the HCl/dioxane method was abandoned without further analysis.

It is widely known that TFA in conjunction with mediators such as anisole or thioanisole is effective for the removal of *tert*-butyl and *t*-butoxycarbonyl (BOC) groups in the synthesis of polypeptides.[20] The function of these mediators has been illustrated by the reaction scheme proposed by Lundt and co-workers.[21] Thioanisole scavenges the *tert*-butyl or BOC carbocations formed during the elimination reaction thus preventing these active groups from attacking vulnerable aromatic residues such as tyrosine and tryptophan, which can ultimately lead to unwanted butylation of these residues (Scheme 3).[22] Deprotection of A-m-PTBMA in the presence of an excess of thioanisole gave >99% elimination of *tert*-butyl groups and ~100% intact anthracene residues.

III. Steady-State Quenching. *a. Stern−Volmer Analysis of Quenching.* The steady-state fluorescence spectra of A-m-PMA as a function of added Tl^+ is shown in Figure 2a. A distinct overall red-shifting of the spectrum as well as a partial loss of vibrational structure with addition of quencher is observed. This spectral shift can be clearly seen in the normalized spectra at

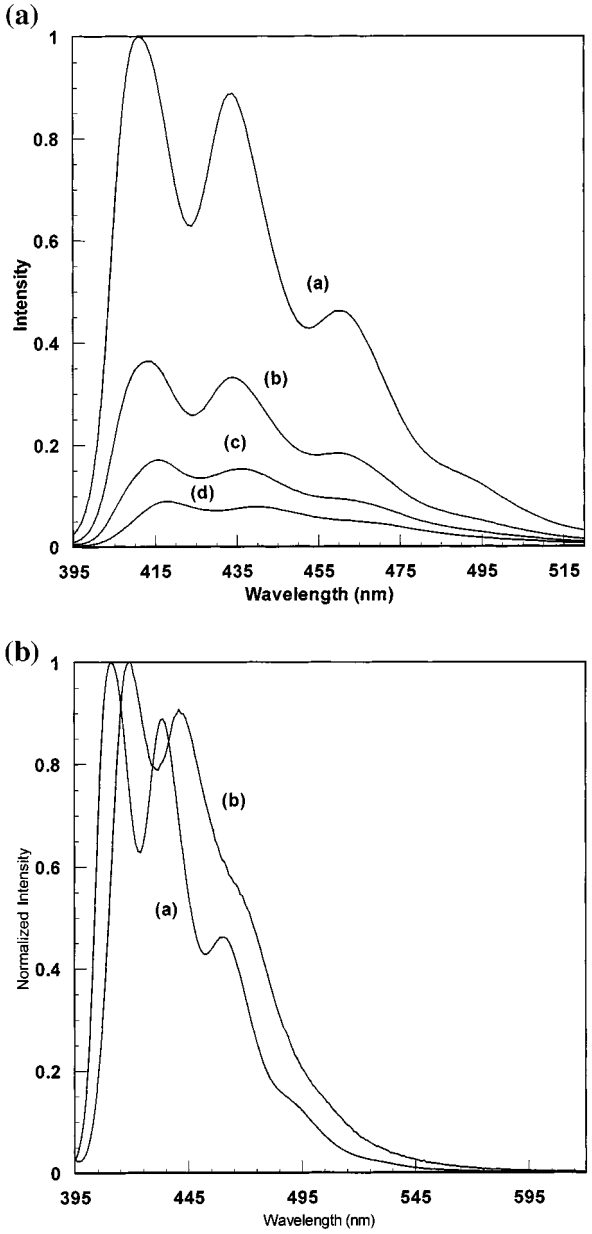

Figure 2. (a) (upper) Steady-state fluorescence spectra of A-m-PMA at [Tl^+] values as follows: (a) 0; (b) 0.131 mM; (c) 0.392 mM; (d) 1.604 mM. (b) (lower) Normalized steady-state fluorescence spectra of A-m-PMA for [Tl^+] = 0 (a) and 11.2 mM (b) (I_0/I = 1 and 14.97, respectively).

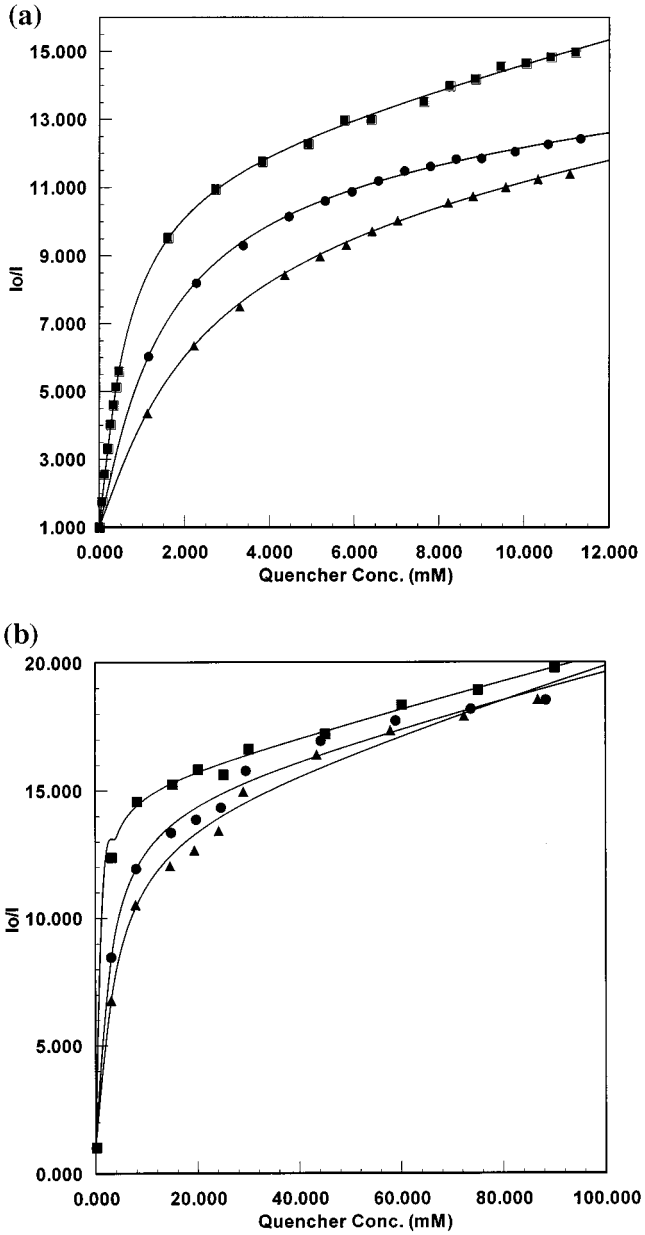

Figure 3. (a) I_0/I plot vs Tl^+ concentration up to 12 mM for the following initial ionic strengths (top to bottom): 1.83 mM (squares); 6.36 mM (circles); 14.83 mM (triangles). (b) Like (a) except maximum Tl^+ concentration 90 mM with the following initial ionic strengths (top to bottom): 1.19 mM (squares); 10.85 mM (circles); 18.28 mM (triangles). In both cases the smooth line is the best fit to the modified Morishima model (eq 10). See Table 3 for the derived parameters.

two different Tl^+ concentrations (Figure 2b). The intensity values used in the SV quenching analysis were obtained from the integral of the spectrum from 395 to 520 nm. An analogous spectral shift was not observed by Morrison et al. for 9-ethanolanthracene pendant-tagged to poly(methacrylic acid) (9EA-PMA).[2] According to the fit of our data to the hindered access model (see later), ca. 5% of the chromophores are "inaccessible" to the Tl^+ quencher. We speculate that if this inaccessibility is real, and not just an artifact of the model, then it may arise as a result of a particular polymer tacticity in the vicinity of the chromophore. We will argue later that Tl^+ binds preferentially in the vicinity of the anthracene chromophore. If so, the spectral shift may be induced by the Tl^+ ion for a subset of chromophores that are not quenched completely.

The quenching data are expressed as the ratio of the fluorescence intensity in the absence of quencher (I_0) to that in the presence of quencher (I) plotted as a function of quencher concentration, i.e., the well-known Stern−Volmer (SV) plot. The nonlinear SV expression for fluorescence quenching is given as

$$I_0/I = 1 + K_{sv}[Q] + A_1[Q]^2 \qquad (2)$$

where [Q] is the quencher concentration. In our use of eq 2 A_1 is an empirical coefficient representing the deviation from SV linearity and K_{sv} is the SV constant.[23] At low quencher concentrations, the higher order SV term is negligible and the SV constant can be calculated from the initial slope of the data. The apparent second-order quenching rate constant, k_q, can be extracted from the defining relationship $K_{sv} = k_q\langle\tau_0\rangle$, where $\langle\tau_0\rangle$ is the fluorescence lifetime in the absence of quencher.

Figure 3a shows the dependence of the SV data on the ionic strength of the solution for [Tl^+] up to 12 mM. From the initial

TABLE 1: Stern−Volmer Analysis of Initial Slope of I_0/I

polymer	IS (mM)	$10^{-3}K_{sv}$ (M^{-1})	$10^{-11}k_q$ (M^{-1} s^{-1})
A-m-PMA[a]	1.83	12.2	14.2[c]
A-m-PMA[a]	6.63	7.40	6.92
A-m-PMA[a]	14.83	3.56	3.33
9EA-PMA[b]	1.91	11.3	9.41[d]

[a] Data from Figure 3a for A-m-PMA. [b] Data from ref 2. [c] $\tau_0 = 10.7$ ns. [d] $\tau_0 = 12$ ns.

slope of the quenching data in the absence of added salt (background IS = 1.83), K_{sv} was found to be 12 220 M^{-1}. Using the value $<\tau_0> = 10.7$ ns (see later section), the quenching rate constant was found to be 1.42×10^{12} M^{-1} s^{-1}. This value compares reasonably well with that of 9EA-PMA at pH 11.00, IS = 1.91 mM, for which k_q was found to be 9.41×10^{11} M^{-1} s^{-1}. The values of K_{sv} and k_q for different ionic strengths are presented in Table 1.

As in the previous work, addition of salt to the solution decreases the magnitude of quenching at all quencher concentrations. This phenomenon can be interpreted in two ways. First, the excess counterions reduce the effective electrostatic attraction of the polyanion for the quencher ion through Debye shielding. Second, the addition of excess counterions may displace quencher ions within the vicinity of the polyelectrolyte. We have referred to this as "statistical dilution" in our earlier paper.[2]

The results for very high quencher concentrations (up to 90 mM) are presented in Figure 3b. As in the earlier work, there is very strong negative curvature for $[Tl^+] > 10$ mM. For the highest Tl^+ concentration there is essentially no effect of added salt and the limiting slope corresponds to $k_q = 4.4 \times 10^9$ M^{-1} s^{-1}, very close to the expected value for a diffusion-limited reaction (see below). In all plots the solid line is the best fit to the modified Morishima model discussed later.

Previous work has shown that increasing the ionic strength of the solution has no effect on quenching by the neutral species acrylamide.[3] Similarly we find for acrylamide quenching of A-m-PMA K_{sv} values of 16.0, 15.4, and 14.7 M^{-1} for IS values of 1.65 (background), 9.28, and 16.6 mM, respectively ($k_q = 1.50-1.37 \times 10^9$ M^{-1} s^{-1}). Although the SV constant does decrease slightly with ionic strength, the effect is small compared to that for the Tl^+ quencher suggesting that the polyanion does not undergo any significant local conformational changes as a consequence of high IS that would provide protection for the anthracene chromophore.

The diffusion-controlled reaction rate (k_{Diff}) between neutral species B and C, with radii r_B and r_C and diffusion rates D_A and D_C, is given by the Smoluchowski expression:

$$k_{Diff} = 4\pi N_A(r_B + r_C)(D_B + D_C) \tag{3}$$

Here N_A is Avogadro's number. For Tl^+ and anthracene reactants we have previously estimated from space-filling models that $r_B + r_C = 8.52$ Å.[2] From the mobility of Tl^+ it is found that $D_{Tl^+} = 2.00 \times 10^{-5}$ cm^2/s,[24] and if we assume that only Tl^+ contributes to D because anthracene is bound to the polyelectrolyte, then the diffusion-controlled rate constant for quenching in water at 25 °C is calculated to be 1.29×10^{10} M^{-1} s^{-1}. For spherical species the diffusion rate is often estimated from the Stokes−Einstein expression, $D = kT/6\pi\eta r$, where η is the solvent viscosity. Using this relation, k_{Diff} for water at 25 °C is 3.5×10^9 M^{-1} s^{-1} for one immobile species. Therefore we expect the diffusion-limited rate to be in the range $(0.35-1.3) \times 10^{10}$ M^{-1} s^{-1}. These values are on the order of 2 orders of magnitude lower than the observed rate constant, demonstrating the overwhelming effect of the electrostatic potential of the polyelectrolyte in concentrating the thallium quencher ion around the probe.

The Coulombic force between point charges is accounted for by the multiplication of k_{Diff} by the Debye term.[25]

$$W/(e^W - 1) \tag{4a}$$

where

$$W = z_B z_C e^2/(4\pi\epsilon_0\epsilon kT[r_B + r_C]) \tag{4b}$$

In eq 4b z_B and z_C are the formal charges on species B and C, e is the proton charge, ϵ_0 is the permittivity of free space, ϵ is the solvent dielectric constant, k is Boltzmann's constant, and T is temperature. For monovalent ions of opposite charge the electrostatic correction is a factor of 1.478. The formal charge on the anthracene reactant must equal 113 in order to yield the quenching rate constant observed for A-m-PMA at low quencher concentrations, which corresponds to approximately half the total formal charge of the polyanion.

At higher quencher concentration (Figure 3b) the I_0/I data roll over and approach a constant slope on the order of 48 M^{-1} for all IS values studied, giving an apparent quenching constant on the order of 4.5×10^9 M^{-1} s^{-1} in good agreement with the value of 2.92×10^9 M^{-1} s^{-1} for 9EA-PMA.[2] These values are very similar to the diffusion-controlled limit discussed above. This is a point we will return to later in the text.

b. Inaccessible Fluorophores: Hindered-Access Model. The negative deviation from linearity in the SV plot (Figure 3) suggests that a fraction of probes are inaccessible to quencher ions. In such cases a two-state model is often employed in which the population of probes is divided into an accessible fraction, f_a, and an inaccessible fraction, f_b, ($f_b = 1 - f_a$). In the usual application of this model it is assumed that as quencher is added to the system the fluorescence intensity of the accessible probes decreases according to the linear SV relation (e.g. eq 2 with $A_1 = 0$; we denote the SV constant for the accessible probes by K_{sv}^a) while the fluorescence intensity of the b probes remains unchanged. This yields the following expression:[23]

$$I_0/(I_0 - I) = 1/f_a + 1/(K_{sv}^a f_a[Q]) \tag{5}$$

where $I_0 = I_{0a} + I_{0b}$. Therefore, a plot of $I_0/(I_0 - I)$ vs 1/[Q] should yield a linear function in which f_a can be obtained from the intercept and K_{sv}^a from the ratio of the intercept and slope. By fitting the data to this model (Figure 4), we obtain quenching rate constants in fair agreement with the values obtained from the initial slope of the SV plot. The fraction of accessible probes is 0.93−0.95 for three different ionic strengths (Table 2). Once again, this result is similar to 9EA-PMA for which f_a was calculated to be 0.95.[2] These findings are consistent with the insensitivity of the neutral quencher acrylamide to ionic strength (see earlier discussion). The persistence length of fully neutralized PMA in aqueous solution (Na^+ counterion) has been found to be 420 Å through electric permittivity measurements.[26] It is difficult to envision the complete encapsulation of a probe species by flexible segments of the chain, thereby rendering them inaccessible to quencher ions. Upon closer inspection of the fit, we find that this model linearizes the data fairly well in the case of excess salt but fails in the absence of excess salt. Therefore, we believe this model is not really appropriate for the present system.

c. Combined Stern−Volmer and Perrin (Morishima) Analysis. For quenching by counterions that are condensed within the vicinity of a polyelectrolyte, the concept of a sphere-of-action

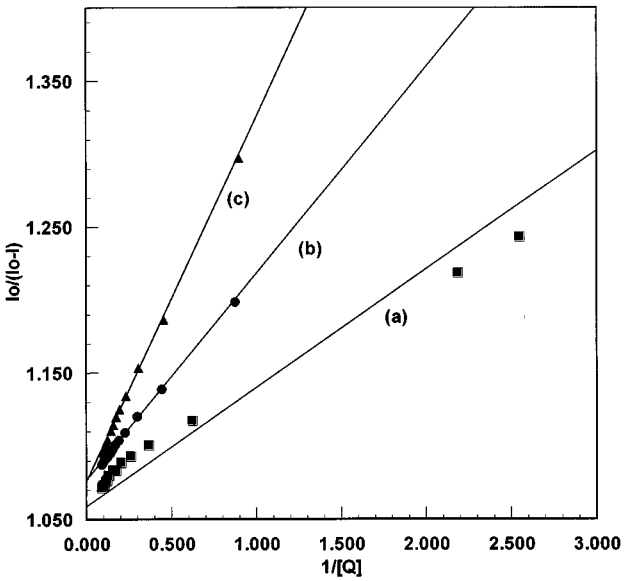

Figure 4. Fit of the data of Figure 3a to the hindered access model. The following identify the initial ionic strength: 1.83 mM (a); 6.36 mM (b); 14.83 mM (c).

TABLE 2: Parameters from Fitting Data of Figure 3a to Hindered Access Model[a]

IS (mM)	$10^{-3}K_{sv}$ (M^{-1})	f_a	IS (mM)	$10^{-3}K_{sv}$ (M^{-1})	f_a
1.83	13.0	0.945	14.83	4.30	0.930
6.63	7.61	0.929			

[a] Equation 5.

quenching (Perrin model) was invoked by Morishima et al.[4b] For the Perrin model quenchers residing within a quenching sphere of action immediately surrounding the probe have a quenching probability equal to unity.[23,27] It is assumed that the probability of finding n quenchers within this spatial region can be described by a Poisson distribution, $P(n) = \exp(-\langle n_Q\rangle)\langle n_Q\rangle^n/n!$, where $\langle n_Q\rangle$ is the average number of quenchers that reside within the volume. Therefore, the probability that the probe will not be quenched is equal to $P(0)$ ($= \exp(-\langle n_Q\rangle)$).[28] In contrast, quenchers that reside outside the condensation zone are assumed to quench by a dynamic mechanism. The quenching reaction involving these so-called "atmospheric" quenchers is assumed to be well described by SV kinetics. In polyelectrolyte systems both mechanisms are expected to be operative such that quenching can be described by a combined Perrin and Stern−Volmer mechanism. An expression incorporating this idea was originally proposed by Morishima et al.[4b]

$$I_0/I = (1 + K_{sv,app}[Tl^+]_{atm}) \exp[\langle n_Q\rangle] \quad (6)$$

where $K_{sv,app}$ is the "apparent" SV constant, $[Tl^+]_{atm}$ is the "atmospheric concentration" of Tl^+, and $\langle n_Q\rangle$ is the average number of quencher ions in the active quenching sphere of the chromophores. In the original model $\langle n_Q\rangle$ is related to the ratio of condensed counterions to fluorophores through an adjustable parameter, α, which represents the fraction of condensed counterions that are in proximity to the fluorescent probe:

$$\langle n_Q\rangle = \alpha C_b/[anth]_0 \quad (7)$$

In this expression, $[anth]_0$ is the bulk concentration of anthracene probes and C_b represents the concentration of bound counterions and is given by simple Manning condensation theory.

TABLE 3: Analysis of Quenching Data Using the Modified Morishima Model (eq 10)

polymer	IS (mM)	$K_{sv,app}$ (M^{-1})	$\langle N\rangle$	K_b
A-m-PMA (Figure 3a)	1.83	26.2[a]	2.50	12.6
	6.63	9.38[a]	2.52	15.0
	14.8	17.4[a]	2.42	20.8
A-m-PMA (Figure 5a)	5.37	17.6	2.48	15.5
A-m-PMA (Figure 3b)	1.94	3.49	2.72	7.75
	11.6	3.42	2.71	13.9
	20.9	4.39	2.66	17.4
9EA-PMA[b]	1.91	3.06	2.76	7.72

[a] $K_{sv,app}$ values from Figure 3b are considered to be more reliable because there are more data points in the concentration region where diffusive quenching dominates. [b] Data from Figure 3 of ref 2. Note that the values quoted in this reference are average ionic strengths, including the addition of quencher.

In our application of the Morishima model we assume that the number of ions that reside near the chromophore is fixed ($\langle N\rangle$) and when quencher ions are added the average number of quenchers is given by $\langle N\rangle x_Q$, where x_Q is the mole fraction of quencher ions. This assumption is in the spirit of Manning condensation theory[29] and also was the basis of a simplified Poisson−Boltzmann model applied earlier.[3] x_Q is computed on the basis of the total concentration of all cations, but if the quencher ion is preferentially bound to the polyelectrolyte or the region near the chromophore, the apparent value of the quencher mole fraction may be higher that the value obtained from using the bulk concentrations of all ions. We will encounter this situation in our data fits. Thus we obtain our modification of the Perrin expression in the absence of preferential binding:

$$I_0/I = (1 + K_{sv,app}[Tl^+]_{atm}) \exp[\langle N\rangle(x_{Tl^+})] \quad (8)$$

Here

$$(x_{Tl^+}) = [Tl^+]_0/([Tl^+]_0 + [K^+]_0) \quad (9)$$

and the subscript 0 denotes bulk concentrations. Equation 8 displays negative curvature in the plot of I_0/I vs $[Tl^+]$. If there is preferential binding of the Tl^+ near the chromophore this can be accounted for by replacing $[K^+]_0$ by $[K^+]_0/K_b$ (see the Appendix). Assuming that $[Tl^+]_{atm} \sim [Tl^+]_0$, our fitting function becomes

$$I_0/I = (1 + K_{sv,app}[Tl^+]_0) \exp\left[\langle N\rangle\left\{\frac{[Tl^+]_0}{[Tl^+]_0 + [K^+]_0/K_b}\right\}\right] \quad (10)$$

with the fitting parameters $\langle N\rangle$, K_b, and $K_{sv,app}$. Equation 10 failed to fit the data satisfactorily unless K_b was allowed to vary. The K_b values obtained from this fit have an average value of ca. 16 but vary with the total ionic strength over the range 12−21 (Table 3). The values of $\langle N\rangle$ obtained from this fit are remarkably constant. The $K_{sv,app}$ values obtained from the fit to the data in Figure 3b are considered more reliable because of the larger number of data points in the saturation region. We note that all the parameters obtained are in reasonable agreement with those of 9EA-PMA (Table 3).

d. Tl^+ Displacement Experiment. Morishima et al. have used a displacement method to assess competitive binding between Tl^+ and other monovalent ions such as Li^+, Na^+, and K^+.[4d] For the present system the Tl^+ displacement experiment was performed by first measuring the fluorescence intensity corresponding to 3.75 mM Tl^+ (IS = 5.37, $I_0/I = 11.5$) and then measuring this value as a function of added excess KNO_3 up to

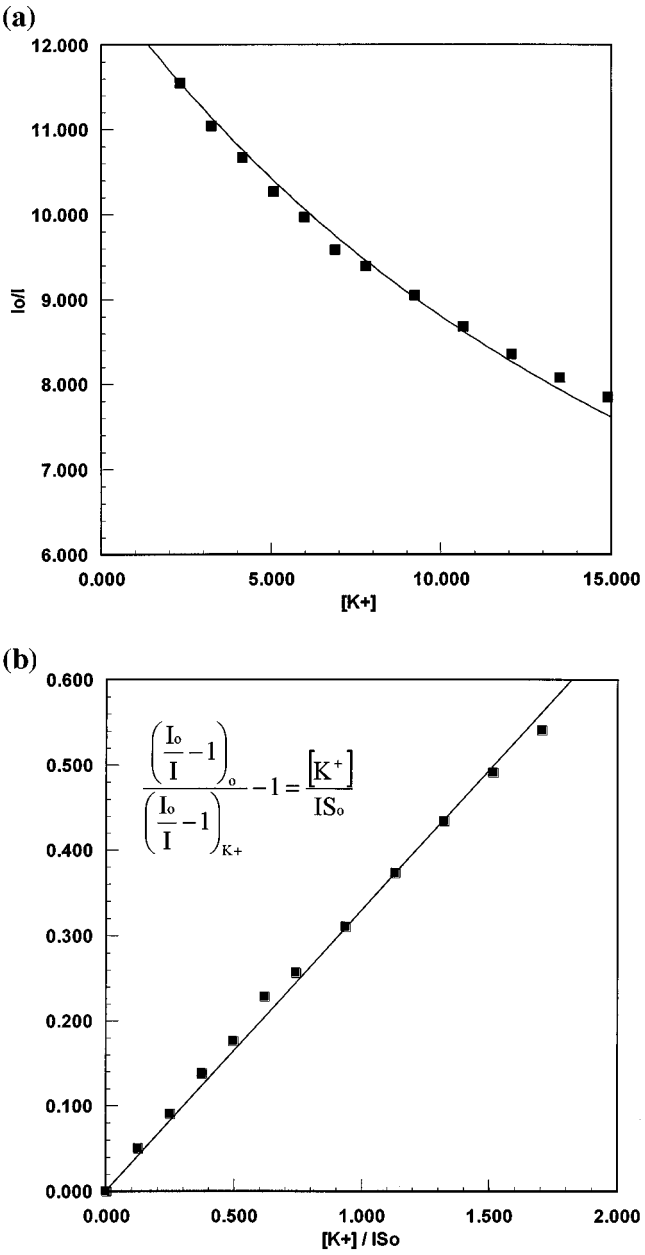

Figure 5. (a) I_0/I vs added K^+ for $[Tl^+] = 3.704$ mM, initial ionic strength 5.37. The smooth line is the fit to the modified Morishima model (eq 10). (b) Data for the displacement experiment plotted according to eq 11. The linear fit yields $\beta = 0.329$. Also shown is the calculation from the modified Morishima model (see text).

14.88 mM (IS = 15.65, $I_0/I = 8$) (see Figure 5a). If these data are fit to eq 10, we obtain fitting parameters in good agreement with those obtained from a normal quenching experiment (see Table 3).

In our earlier paper in which a displacement experiment was analyzed, we started with the simple linear Stern−Volmer expression and wrote $[Tl^+] = cx_{Tl^+}$, where c is the total concentration of cations. From this, one can propose the following expression as a measure of preferential binding:[3]

$$\frac{(I_0/I-1)_0}{(I_0/I-1)_{K^+}}-1=\beta\frac{[K^+]_{excess}}{IS_0} \qquad (11)$$

Here the subscript 0 refers to the solution before the addition of excess K^+. $[K^+]_{excess}$ corresponds to the additional K^+ added during the displacement experiment, and IS_0 is the initial total ionic strength, including the quencher ion. In the case of simple SV quenching the slope (β) should be unity. Figure 5b shows the data plotted in this fashion, which has a slope of 0.329. The modified Morishima model with $K_b = 16.1$ (the average value of all determinations) also yields a plot that is essentially linear and matches experiment very well.

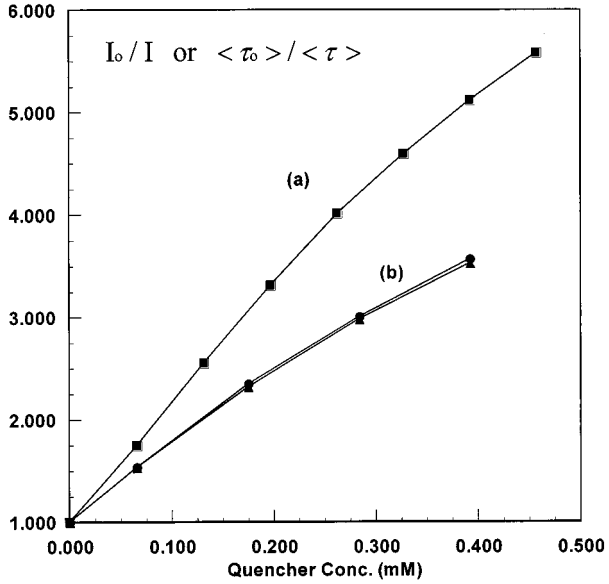

Figure 6. Steady-state (curve a) and time-resolved (curve b) quenching of A-m-PMA. The circles and triangles in curve b correspond to a double and triple exponential fit to the decay curve.

III. Time-Resolved Quenching. The lifetime and steady-state quenching of A-m-PMA are compared in Figure 6. Due to signal-to-noise limitations, the lifetime measurements were limited to relatively low quencher concentrations. The fluorescence decays were fit to the sum of exponentials:

$$I(t) = \sum_i \alpha_i \exp(-t/\tau_i) \qquad (12)$$

Here $I(t)$ is the fluorescence intensity as a function of time (normalized to unity at $t = 0$) and α_i and τ_i are the preexponential factor and lifetime of the ith component, respectively. We define the average lifetime as

$$<\tau> = \sum_i \alpha_i \tau_i \qquad (13)$$

$<\tau>$ represents the integral of $I(t)$ from 0 to ∞, which is directly comparable to the steady-state intensity.[30] The fluorescence lifetime in the absence of quencher, $<\tau_0>$, was determined to be 10.7 ns (essentially equal to the 12.0 ns for 9EA-PMA).

The lifetime quenching is characterized by the value of $<\tau_0>/<\tau>$. As can be seen from Figure 6 (curve b), these results are unchanged using a two- or three-exponential fit. If there is an element of "static quenching" (i.e. a quenching process faster than we can measure), then we expect $<\tau_0>/<\tau>$ to lie below I_0/I.[31] We should note that the models we used to fit the data in the previous sections do not directly calculate the dynamics of quenching but rather the integral of $I(t)$.

The α_i, τ_i data are given in Table 4. We note that the unquenched decay is well-described by a single exponential ($\alpha_1 = 0.991$) and in fact in all cases the fluorescence decay is only modestly nonexponential. The nonexponentiality is more pronounced as quencher is added ($\alpha_1 = 0.838$ at $[Tl^+] = 0.392$ mM). After addition of quencher and analysis of the fluorescence lifetime, K^+ was added to the system and the effect on the life-

TABLE 4: Results from Fitting Fluorescence Decay to Two Exponentials

$[Tl^+]$ (mM)	IS (mM)[a]	τ_1 (ns)	α_1	τ_2 (ns)	α_2	$<\tau>_0$
0.0	1.83	10.76	0.991	0.37	0.009	10.70
0.066	1.97	7.22	0.956	0.93	0.044	6.94
0.175	2.21	5.04	0.867	1.22	0.133	4.53
0.284	2.45	4.09	0.812	1.15	0.188	3.54
0.392	2.68	3.39	0.838	0.78	0.162	2.97
0.388	6.69	4.60	0.857	1.19	0.143	4.11
0.384	10.61	5.36	0.893	1.26	0.107	4.92
0.379	14.44	5.91	0.924	1.06	0.076	5.54

[a] In this table the value of IS given is the sum of the Tl^+ plus background and added salt.

time was monitored. It was found that the decay is slightly more exponential ($\alpha_1 = 0.838$ and 0.924 for IS = 2.68 and 14.44 mM, respectively). This can be rationalized as the result of excess K^+ displacing Tl^+ from the region of the chain, which decreases the static-quenching component. This is qualitatively similar to results obtained for other polymer systems for which single photon counting methods were used to obtain the lifetime data.

In contrast, our earlier work on 9EA-PMA shows almost only dynamic quenching throughout the entire quenching range even though both steady-state and time-resolved quenching curves both strongly deviate from linearity at higher Tl^+ concentrations.[32] The relative importance of static quenching for A-m-PMA is the most significant difference we have found between these two polymer systems. We presume that this a consequence of the point of chromophore attachment and not an instrumental artifact (e.g. the difference between single photon and phase modulation time-dependent fluorescence measurements).

Discussion

To achieve a better understanding of the role of ionic strength in the quenching process it is helpful to discuss Manning's counterion condensation theory.[33] The effects of polyelectrolytes on a number of chemical reactions have been explained quite well within the basic framework of the model. According to Manning, polyelectrolytes in solution can be characterized by a charge density parameter ξ, given by

$$\xi = \frac{e^2}{\epsilon kTb} \tag{14}$$

where e, ϵ, k, and T have been defined previously and b is the average axial spacing between charged groups on the polyelectrolyte. The critical charge density parameter is defined as $\xi_c = N^{-1}$, where N is the charge of the counterion. When $\xi > \xi_c$, counterions will condense on the polyelectrolyte until the effective charge density parameter equals ξ_c. For $\xi < \xi_c$ no condensation occurs. For fully ionized PMA $\xi = 2.8$ ($b = 2.55$) and it is predicted that condensation of monovalent ions proceeds until $(1 - \xi^{-1}) = 0.64$ of the total polymer charge has been effectively neutralized. Excess monovalent ions added to the system may freely exchange with previously condensed species, but the net population of condensed counterions remains the same. The concentration of counterions remains constant from the surface of the polyelectrolyte to a radius that is a function of the linear change density and ξ. We have previously estimated the radius of the condensation zone to be 16.3 Å for PMA.[3,29]

One of the motivations for carrying out the present synthetic approach was to compare the fluorescence quenching of an in-chain anthracene probe (A-m-PMA) with previous work from this laboratory using a pendent chromophore (9EA-PMA). In the context of a charged cylinder model (Scheme 4) one might expect to see different ion distributions and/or transport for these

SCHEME 4

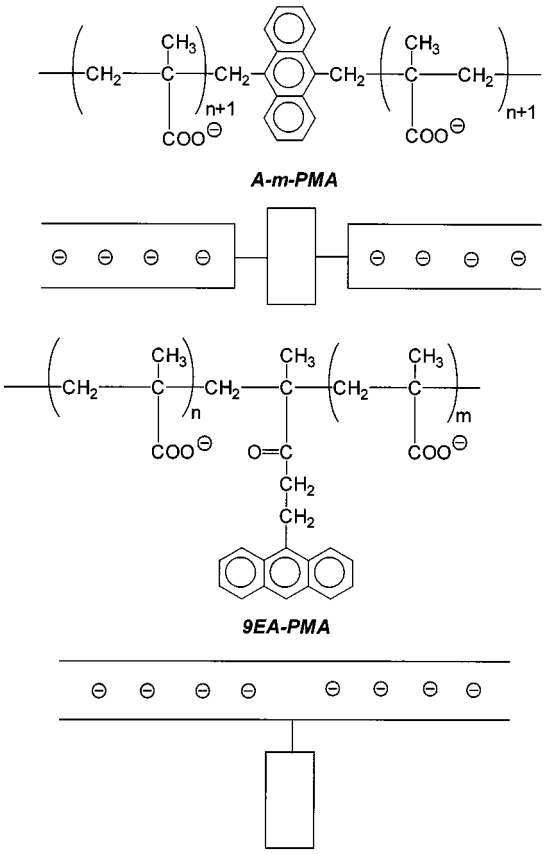

two cases. In fact most aspects of the fluorescence quenching are essentially identical for these two systems. According to our estimate of the thickness of the condensation zone (16.3 Å; see above), it is reasonable that both anthracene probes would experience similar ion densities and therefore be quenched equivalently. A similar conclusion was reached by Morishima et al. on the basis of studies of a pH-dependent merocyanine dye attached to poly(acrylic acid)-*co*-acrylamide.[34] The only significant difference we have found is that static quenching is more important for the in-chain case, which suggests that the density of quenching ions in the immediate vicinity of the chromophore is somewhat higher.

If most quenching events originate from Tl^+ ions that are condensed on the polyelectrolyte, and if the concentration of condensed ions is constant, then in the absence of preferential binding all quenching processes should depend on the mole fraction of Tl^+ with respect to all monovalent cations.[35] This is in contrast to classical homogeneous quenching processes in which it is the molar concentration of quenchers that determines the rate of quenching. In the present work the plots of I_0/I vs x_{Tl^+} almost superimpose (Figure 7) as was the case for 9EA-PMA (ref 2, Figure 8). There is a slight positive displacement for higher ionic strengths which can be the result of the following: (1) preferential binding of the Tl^+ ion in the vicinity of the probe; (2) a contribution to the quenching via a homogeneous mechanism for which the quenching is proportional to $[Tl^+]$ and not x_{Tl^+}. We note the relation

$$[Tl^+] = IS_0 \frac{x_{Tl^+}}{1 - x_{Tl^+}} \tag{15}$$

where IS_0 is the initial ionic strength of the solution before the addition of Tl^+. Therefore a positive displacement is expected

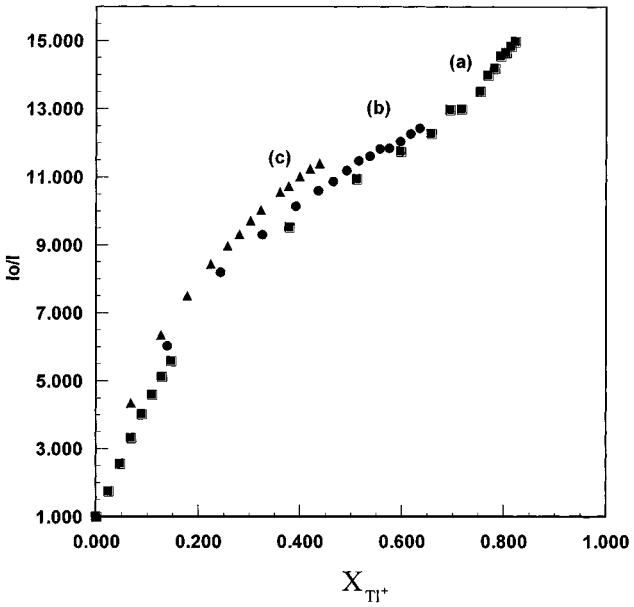

Figure 7. Plot of I_0/I as a function of x_{Tl^+} for the following initial ionic strengths: curve a, 1.83 mM (squares); curve b, 6.36 mM (circles); curve c, 14.83 mM (triangles) (from the data of Figure 3a).

if homogeneous quenching is important. However, for all fits to the Morishima model the homogeneous quenching term ($1 + K_{sv,app}[Tl^+]_0$) in eq 10 makes a relatively small contribution to the overall quenching.

In our previous work we measured the preferential binding of Tl^+ to homopolymer PMA and found binding constants relative to K^+ or Na^+ on the order of 1.4.[3] This is not necessarily the same binding constant obtained by fits our modification of the Morishima model (eq 10) which reflects preferential binding in the immediate vicinity of the probe. This model fits our data very well, but of course it has three adjustable parameters. The physical picture is strongly influenced by the Manning model. As quencher is added, the fixed number of condensed ions ($\langle N \rangle$) near the fluorophore are replaced by Tl^+. If K_b in eq 10 is greater than unity, then Tl^+ replaces the K^+ counterions more efficiently than expected on the basis of mole fraction alone. K_b is found to be higher than for bulk PMA (cf. 1.4 and 12−20) so there must be a favorable interaction of Tl^+ with the aromatic chromophore or the lower charge density near the chromophore somehow favors Tl^+.

In our earlier work the physical picture proposed by Morishima et al. stimulated us to consider a simplified model for the quenching of a fluorophore covalently bound to a polylelectrolyte, which we referred to as the "tube model".[3] For this model, reaction-diffusion equations were solved for a constant concentration of ions confined to the immediate vicinity of the polyelectrolyte. Because one must carry out numerical integration of the diffusion-reaction equations for specific geometric parameters, this model is hard to apply for data-fitting purposes. Many of the features of the tube model are very similar to the modified Morishima model (e.g. rollover in I_0/I at high quencher concentration, the effect of preferential binding on the ionic strength dependencies). While a quantitative fit to experimental data was not attempted in ref 3, the qualitative behavior of the data suggested that preferential binding had to be evoked. In the present experiments the value of K_b obtained by fitting different experimental data sets is in reasonable agreement for A-m-PMA and approximately a factor of 2 higher than for 9EA-PMA (Table 3). We believe that the conclusion that there is preferential binding of Tl^+ near the chromophore is inescapable.

At high Tl^+ concentration the slope of I_0/I is greatly diminished. Note that the maximum value of I_0/I produced by condensed ion quenching is $e^{\langle N \rangle}$. The additional quenching is by noncondensed ions that diffuse into the region of the chromophore and is described by the $1 + K_{SV,app}[Tl^+]$ factor in eq 10. The $K_{SV,app}$ values extracted from the Morishima model are approximately 10^3 lower than the initial slope of the Stern−Volmer plot and correspond approximately to a second-order reaction rate between neutral species, one of which is immobile. This is very much in keeping with the physical picture described above.

Summary

A detailed procedure for the synthesis and tagging of anthracene mid-tagged poly(methacrylic acid) has been described that includes an effective deprotection route that does not destroy the attached anthracene probe.

The steady-state and time-resolved fluorescence quenching of A-m-PMA by Tl^+ have been obtained and analyzed using several different models. The data are very similar to that observed for the anthracene pendant-tagged system 9EA-PMA studied by Morrison et al.[2] According to the two-state or hindered-access model, the fluorophore populations for both systems appear to be largely accessible by quenchers even at high ionic strengths. However this model is not believed to be appropriate because of the relatively poor fit at low ionic strength.

The primary effect of ionic strength on the quenching process was found to be statistical dilution of Tl^+, as was observed for 9EA-PMA. However, analysis of several aspects of the data have suggested that there is preferential binding of Tl^+ near the chromophore. Our previous attempts to understand the degree of preferential binding using a more complex model did not lend themselves to fitting experimental data.[3] In contrast, modification of the model proposed by Morishima does allow a fitting procedure. Using this model, preferential binding constant values (K_b) of ∼12−21 were found for A-m-PMA at the different ionic strengths studied while a value of ∼7 was found for 9EA-PMA. While the precise numerical value should not be taken too seriously, we believe that the preponderance of evidence is consistent with preferential binding of Tl^+ near the anthracene chromophore.

Time-resolved measurements demonstrated that as quencher is added to the system, the magnitude of static quenching increases. Static quenching is diminished by the addition of salt. Similar observations were made for 9EA-PMA with the important difference that static quenching is much less pronounced than for A-m-PMA. This was found to be the most significant difference between the two systems. For A-m-PMA the nearly single exponential character of the fluorescence decay persists even in the presence of quencher. This suggests to us that within the condensation zone of the counterions the concentration is relatively uniform and that the condensation zone is significantly larger than the anthracene probe. Therefore the lifetime quenching is similar to that obtained in homogeneous solution at a comparable Tl^+ ion concentration.

The objective of this work has been to understand the dependence of fluorescence quenching on the position of the probe with respect to the backbone of the polyelectrolyte. From this we are beginning to obtain a more sophisticated three-dimensional view of the distribution of quencher and other counterions about the polyelectrolyte. Future work will address polyelectrolyte end-effects on quenching reactions.[36]

Acknowledgment. This research has been supported by the Office of Naval Research (Grant N00014-91-J-1667) and the Robert A. Welch Foundation (Grant F-356). This support is gratefully acknowledged. The authors also wish to thank Prof. G. C. Willson for many helpful discussions regarding the deprotection procedure including the critical suggestion that thioanisole could be used to prevent destruction of the anthracene moiety.

Appendix

We consider the Tl^+ and K^+ ions to compete for binding in the region of space near the chromophore. The preferential binding of the Tl^+ can be expressed by the equilibrium

$$Tl^+(aq) + K^+(b) = Tl^+(b) + K^+(aq) \qquad \text{(A-1)}$$

$$\frac{[Tl^+(b)][K^+(aq)]}{[Tl^+(aq)][K^+(b)]} = K_b \qquad \text{(A-2)}$$

where b refers to an ion bound in the sphere of action and aq refers to an ion in bulk solution. The region of space around the chromophore is small, so the fraction of all Tl^+ or K^+ ions bound in the region is also small. Therefore we may write

$$\frac{[Tl^+(b)]}{[K^+(b)]} = K_b \frac{[Tl^+(aq)]_0}{[K^+(aq)]_0} \qquad \text{(A-3)}$$

where $[Tl^+(aq)]_0$ refers to the bulk concentration. Note that K_b is the preferential binding constant specifically for the region near the chromophore and may differ numerically from preferential binding (if any) on the polyelectrolyte chain itself. The ratio of concentrations is equal to the ratio of mole fractions, so

$$\frac{(x_{Tl^+})_b}{(x_{K^+})_b} = \frac{(x_{Tl^+})_b}{1 - (x_{Tl^+})_b} = K_b \frac{(x_{Tl^+})_0}{1 - (x_{Tl^+})_0} \qquad \text{(A-4)}$$

Since

$$(x_{Tl^+})_0 = \frac{[Tl^+]_0}{[Tl^+]_0 + [K^+]_0} \qquad \text{(A-5)}$$

we can substitute into eq A-4 and after some simplification obtain

$$(x_{Tl^+})_b = \frac{[Tl^+]_0}{[Tl^+]_0 + [K^+]_0/K_b} \qquad \text{(A-6)}$$

References and Notes

(1) (a) Taha, I. A.; Morawetz, H. *J. Polym. Sci, Part A-2* **1971**, *9*, 1669. b) Sassoon, R.; Rabani, J. *J. Phys. Chem.* **1985**, *89*, 5500. (c) Delaire, J.; Sanquer-Barrie, M. *J. Phys. Chem.* **1988**, *92*, 1252. (d) Kim, H.; Claude, B.; Tondre, C. *J. Phys. Chem.* **1990**, *94*, 7711. (e) Morishima, Y.; Tominaga, Y.; Kamachi, M. *J. Phys. Chem.* **1991**, *95*, 6027. (f) Sassoon, R.; Hug, G. *J. Phys. Chem.* **1993**, *97*, 7823.

(2) Morrison, M.; Dorfman, R.; Clendening, W.; Kiserow, D.; Rossky, P.; Webber, S. E. *J. Phys. Chem.* **1994**, *98*, 5534.

(3) Morrison, M.; Dorfman, R.; Webber, S. E. *J. Phys. Chem.* **1996**, *100*, 15187.

(4) (a) Morishima, Y.; Higuchi, Y.; Kamachi, M. *J. Polym. Sci.* **1991**, *29*, 677. (b) Morishima, Y.; Ohgi, H.; Kamachi, M. *Macromolecules* **1993**, *26*, 4293. (c) Morishima, Y.; Higuchi, Y.; Kamachi, M. *J. Polym. Sci.* **1993**, *31*, 373. (d) Morishima, Y.; Sato, T.; Kamachi, M. *Macromolecules* **1996**, *29*, 1633. (e) Morishima, Y.; Sato, T.; Kamachi, M. *Macromolecules* **1996**, *29*, 3960.

(5) Hruska, Z.; Vuillemin, B.; Riess, G.; Katz, A.; Winnik, M. *Makromol. Chem.* **1992**, *193*, 1987.

(6) (a) Webber, S. E.; *J. Phys. Chem. B* **1998**, *102*, 2618. (b) Prochàzka, K.; Kiserow, D. J.; Webber, S. E. *Acta Polym.* **1995**, *46*, 277.

(7) (a) Katchalsky, A. J. *Polym. Sci.* **1951**, *7*, 393. (b) Arnold, R. *J. Colloid Sci.* **1957**, *12*, 2689. (c) Leyte, J. C.; Mandel, M. *Polym. Sci., Part A-1* **1964**, *2*, 1879. (d) Morawetz, H. *Macromolecules* **1996**, *29*, 2689.

(8) Allen, R.; Long, T.; McGrath, J. *Polym. Bull.* **1986**, *15*, 127.

(9) Ziegler, K.; Dislich, H. *Chem. Ber.* **1957**, *90*, 1107.

(10) Hruska, Z.; Winnik, M. A.; Hurtrez, G.; Riess, G. *Polym. Commun.* **1990**, *31*, 402.

(11) Golden, J. H. *J. Chem. Soc. London* **1961**, 3741.

(12) Warzelhan, V.; Hocker, H.; Schulz, G. V. *Makromol. Chem.* **1978**, *179*, 2221.

(13) Valeur, B.; Rempp, P.; Monnerie, L. *C. R. Hebd. Seances Acad. Sci. Paris, Ser. C* **1974**, *279*, 1009.

(14) Programs written by Dr. T. J. Martin.

(15) Procedure referenced in Aldrich catalog under the trade name Diazald.

(16) Sasaki, T.; Yamamoto, M.; Nishijima, Y. *Macromolecules* **1988**, *21*, 610.

(17) (a) Long, T.; DePorter, C.; Patel, E.; Dwight, D.; Wilkes, G.; McGrath, J. *Polym. Prepr.* **1987**, *28*, 214. (b) Deporter, C.; Long, T.; Venkateshwaran, L.; Wilkes, G.; McGrath, J. *Polym. Prepr.* **1988**, *29*, 343.

(18) Kamachi, M.; Kurihara, M.; Stille, J. *Macromolecules* **1972**, *5*, 161.

(19) Procházka, K.; Kiserow, D.; Ramireddy, C.; Tuzar, Z.; Munk, P.; Webber, S. E. *Macromolecules* **1992**, *25*, 454.

(20) (a) Kemp, D.; Fotouhi, N.; Boyd, J.; Carey, R.; Ashton, C.; Hoare, J. *Int. J. Peptide Protein Res.* **1988**, *31*, 359. (b) Pearson, D.; Blanchette, M.; Baker, M.; Guindon, C. *Tetrahedron Lett.* **1989**, *30*, 2739.

(21) Lundt, B.; Johansen, N.; Volund, A.; Markussen, J. *Int. J. Peptide Protein Res.* **1978**, *12*, 258.

(22) Sieber, P. *Pept., Pro. Eur. Symp., 9th* **1968**, 236.

(23) Lakowicz, J. *Principles of Fluorescence Spectroscopy*; Plenum Press: New York, 1983.

(24) C*RC Handbook of Chemistry and Physics*, 66th ed.; Weast, R., Ed.; CRC Press: Boca Raton, FL, 1985; p D-167.

(25) Levine, I. *Physical Chemistry*, 3rd ed.; McGraw-Hill Book Co.: New York, 1988; p 559.

(26) Van Der Touw, F.; Mandel, M. *Biophys. Chem.* **1974**, *2*, 231.

(27) Birks, J. B. *Photophysics of Aromatic Molecules*; Wiley-Interscience: New York, 1970; p 441.

(28) This is clearly an oversimplifcation because ions in the sphere of action are not necessarily 100% effective at quenching. However, the simple Perrin model captures the main physical features of "contact quenching".

(29) Manning, G. *J. Chem. Phys.* **1969**, *51*, 924.

(30) Webber, S. E. *Photochem. Photobiol.* **1997**, *65*, 33.

(31) See the discussion of static quenching in ref 30. Static quenching may be described operationally as quenching which occurs too quickly to be observed by the time-dependent detection equipment. The phase-modulation SPEX τ2 system is able to detect lifetimes as short as 0.1−0.2 ns, but fitting such a short component along with much longer-lived components is problematic.

(32) See Figure 3 of ref 2.

(33) Anderson, C. F.; Record, M. T. *Annu. Rev. Biophys. Biophys. Chem.* **1990**, *19*, 423.

(34) Morishima, Y.; Higuchi, Y.; Kamachi, M. *J. Polym. Sci, Part A: Polym. Chem.* **1991**, *29*, 677.

(35) In ref 4e the displacement of Tl^+ by divalent ions is discussed.

(36) John Clements, manuscript in progress.